

Tree-aggregated regression for compositional data with measurement errors

Zhengan Li¹ and Tianying Wang^{2*}

¹School of Statistics, University of Minnesota

²Department of Statistics, Colorado State University

Abstract

High-dimensional compositional covariates, often derived from count data, are subject to measurement error and are frequently analyzed after aggregation along a prespecified tree to improve interpretability in applications such as microbiome studies. Existing approaches typically handle either tree-guided compositional regression or errors-in-variables correction, but they do not account for the hierarchical contamination induced by their interaction. We show that tree aggregation turns leaf-level measurement error into level-dependent, correlated contamination across aggregated nodes, which inflates bias, weakens concentration rates for corrected estimating quantities, and leads to unstable variable selection for naive approaches.

We propose Tree-Aggregated Regression with Correction for Observation Error (TARCO), which integrates bias-corrected estimating quantities with a tree-aware positive semidefinite stabilization and sparse regularization, with tuning selected by cross-validation based on the corrected objective. The resulting convex program can be solved with scalable algorithms. We establish finite-sample bounds for prediction and estimation errors and prove sign consistency under conditions that explicitly reflect tree heterogeneity. The guarantees persist when the measurement-error covariance is replaced by a consistent estimator. Simulations across multiple tree depths and a microbiome application demonstrate improved estimation accuracy, support recovery, and aggregation-level interpretability compared with methods that ignore the interaction between tree aggregation and measurement error.

Keywords: Bias correction; Compositional data; Log-ratio transformation; Penalized regression; Tree-structured sparsity.

1 Introduction

Compositional covariates are commonly constructed from count data and therefore inherit non-negligible measurement error from sampling, sequencing, and normalization (Firth and Sammut, 2023; Shi et al., 2022; Tan et al., 2024). In many modern applications, especially microbiome studies, these covariates are also organized on a prespecified biological hierarchy and interpreted after aggregation (Silverman et al., 2017; Bien et al., 2021; Li et al., 2023). This combination creates

*Tianying.Wang@colostate.edu

a central challenge: aggregation improves interpretability, but it also changes how measurement error propagates across levels of the hierarchy.

The consequences of ignoring measurement-error contamination are well documented even in flat high-dimensional compositional regression, where estimation bias and unstable variable selection can arise (Shi et al., 2022; Zhao and Wang, 2024; Tan et al., 2024). Under tree aggregation, the issue becomes more structural: leaf-level contamination is pooled upward, uncertainty becomes level dependent, and group-level summaries can be systematically distorted, as formalized in Section 2.3 and Proposition 1. In other words, the inferential risk is not only larger in magnitude, but also heterogeneous across the hierarchy.

Existing practice typically follows one of two partial routes. One route applies tree-guided compositional regression to observed covariates (Silverman et al., 2017; Garcia et al., 2014; Wang and Zhao, 2017; Randolph et al., 2018; Yan and Bien, 2021; Bien et al., 2021; Li et al., 2023). This preserves hierarchical interpretability, but it can miss measurement-error effects that accumulate across levels. The other route starts from compositional errors-in-variables correction (Shi et al., 2022; Gihawi et al., 2023; Firth and Sammut, 2023; Zhao and Wang, 2024; Tan et al., 2024). This can reduce contamination bias in flat designs, but it does not natively capture how error propagation changes once features are aggregated on a tree.

More importantly, joint handling is not a simple add-on of the two routes above. The target covariate design is latent, while only a contaminated version is observed, so correction must be carried through a structured reparameterization rather than appended afterward. Flat-design correction tools such as CoCoLasso provide an important blueprint (Datta and Zou, 2017). Our guarantees are developed under a random-design setting in which latent log-ratio covariates and their tree-aggregated transforms are stochastic, reflecting sample-to-sample variability in sequencing-based compositional studies. Under hierarchical compositional aggregation, however, the corrected quantities become level dependent, and high-dimensional optimization can still be unstable without additional structural stabilization. This non-additivity appears in both the theory and the toy example, where aggregation depth directly changes error behavior.

This non-additivity is illustrated by the toy design analyzed in Section 2.3 and Section G of the Supplement, where, in this toy setting, naive aggregation can induce spurious nonzero leaf-level estimates even when the true leaf effects are zero. The induced bias is redistributed across levels, with larger shifts toward upper nodes as the number of leaves in a node and measurement-error variance increase. These patterns motivate tree-weighted correction and stabilization as integral

components of the estimator, rather than a post hoc combination of flat-design correction with tree aggregation.

Our methodological goal is to develop a single framework that jointly addresses contamination correction, tree-guided aggregation, and stable high-dimensional fitting. To fill this gap, we propose Tree-Aggregated Regression with Correction for Observation Error (TARCO). Our key message is that, under hierarchical aggregation, measurement-error correction should be built together with the aggregation procedure rather than added afterward. Our contributions are as follows.

1. We quantify how tree aggregation reshapes measurement error and induces level-dependent bias and deterioration in concentration rates. Proposition 1 formalizes this amplification mechanism and shows why higher-level aggregated nodes are intrinsically harder to estimate reliably.
2. Guided by this insight, we develop TARCO as an estimation framework that jointly corrects measurement-error contamination and preserves hierarchical aggregation, together with a tree-aware stabilization step for high-dimensional fitting (Section 2.4).
3. We establish finite-sample prediction and estimation guarantees and prove sign consistency under assumptions that explicitly reflect tree heterogeneity (Section 3). We further show robustness to covariance estimation and demonstrate, through simulations and a microbiome application, that tree-aware correction improves both accuracy and aggregation interpretability relative to naive alternatives.

The relationship to existing frameworks is clarified by two boundary cases. TARCO reduces to a CoCoLasso-type corrected sparse regression when there is no aggregation (i.e., the tree has no internal nodes), and it reduces to tree-guided compositional regression when the measurement error is absent.

The remainder of the paper is organized as follows. Section 2 introduces the model setup, measurement-error formulation, and TARCO estimator. Section 3 presents theoretical guarantees. Sections 4 and 5 report simulations and real-data analysis. The Supplement contains all proofs, additional simulations, application variants, and cross-validation details.

2 Method

We begin with the compositional regression setup, tree parameterization, and the corresponding error-free baseline objective. We then specify the measurement error model, explain why naive tree aggregation fails under contamination, and develop a corrected and stabilized estimator with practical penalty and computation details.

2.1 Model Setup, Tree Parameterization, and Error-free Baseline Objective

Denote by $X = (X_{ij})$ an $n \times p$ compositional data matrix and by $y = (y_1, \dots, y_n)^\top$ an outcome vector, where n and p are the sample size and the number of components, respectively. We use the additive log-ratio (ALR) transformation with the p th component as reference (Aitchison, 1982):

$$Z_{ij} = \log(X_{ij}/X_{ip}) = \log(X_{ij}) - \log(X_{ip}), \quad j = 1, \dots, p-1. \quad (1)$$

The corresponding log-contrast model is (Aitchison and Bacon-Shone, 1984; Lin et al., 2014; Shi et al., 2016)

$$y_i = \sum_{j=1}^{p-1} \beta_j^* Z_{ij} + e_i, \quad i = 1, \dots, n. \quad (2)$$

We extend the ALR design by setting $Z_{ip} = 0$ so that $Z \in \mathbb{R}^{n \times p}$.

Let \mathcal{T} be a prespecified tree with T non-root nodes and leaves $L(\mathcal{T}) = \{1, \dots, p\}$. For each node k , let L_k be its descendant leaf set. Define the aggregation matrix $A \in \{0, 1\}^{p \times T}$ by $A_{jk} = 1$ if node k is an ancestor of leaf j , and 0 otherwise. Then the tree-reparameterized model is

$$y = \sum_{k=1}^T \left(\sum_{j \in L_k} Z_j \right) \gamma_k^* + e = \sum_{j=1}^p Z_j \sum_{k \in \text{ancestor}(j)} \gamma_k^* + e, \quad (3)$$

with $\beta^* = A\gamma^*$.

In the error-free setting, tree-aggregation estimators are based on

$$\mathcal{L}(\beta, \gamma) = \frac{1}{2n} \|y - Z\beta\|_2^2 + \lambda \mathcal{P}(\gamma), \quad \text{subject to } \mathbf{1}_p^\top \beta = 0, \beta = A\gamma, \quad (4)$$

or equivalently

$$\mathcal{L}(\gamma) = \frac{1}{2} \gamma^\top \Psi \gamma - \psi^\top \gamma + \lambda \mathcal{P}(\gamma), \quad \text{subject to } (A^\top \mathbf{1}_p)^\top \gamma = 0, \quad (5)$$

where $\Psi = n^{-1} A^\top Z^\top Z A$ and $\psi = n^{-1} A^\top Z^\top y$.

If measurement error is ignored and the observed design is substituted directly for Z , the same template yields a naive tree-aggregation estimator. We formalize this naive construction in Section 2.3, after introducing the measurement-error model in Section 2.2.

2.2 Measurement Error Model

Let $\tilde{X} = (\tilde{X}_{ij})$ denote the observed corrupted composition matrix. We adopt a multiplicative error model on pre-compositional data:

$$\tilde{R}_{ij} = R_{ij}v_{ij},$$

where R_{ij} denotes the true pre-compositional value for the i th sample and j th feature, and v_{ij} is the multiplicative error. This formulation, common in compositional data analysis (Firth and Sammut, 2023; Tan et al., 2024), preserves non-negativity when multiplicative errors remain positive.

The true compositional data is $X_{ij} = R_{ij}/N_i$, where $N_i = \sum_{j=1}^p R_{ij}$. We observe contaminated compositional data $\tilde{X}_{ij} = \tilde{R}_{ij}/\tilde{N}_i$, where $\tilde{N}_i = \sum_{j=1}^p \tilde{R}_{ij}$. The relationship between true and observed compositional data is

$$\tilde{X}_{ij} = X_{ij}v_{ij}N_i/\tilde{N}_i, \quad j = 1, \dots, p. \quad (6)$$

Applying log-ratio transformations to (6) converts the multiplicative model to an additive form. Given the unit-sum constraint $\sum_{j=1}^p \tilde{X}_{ij} = 1$, we define

$$U_{ij} = \log\left(\frac{v_{ij}}{v_{ip}}\right), \quad j = 1, \dots, p-1. \quad (7)$$

From (6) and (7), we obtain the additive error model

$$\tilde{Z}_{ij} = Z_{ij} + U_{ij}, \quad j = 1, \dots, p-1. \quad (8)$$

We extend this definition by setting $Z_{ip} = U_{ip} = \tilde{Z}_{ip} = 0$. Thus $Z = (Z_{ij})$, $U = (U_{ij})$, and $\tilde{Z} = (\tilde{Z}_{ij})$ are $n \times p$ matrices. We assume that the multiplicative errors v_{ij} are independent of Z_i and e_i (Loh and Wainwright, 2011), and that after the log-ratio transformation, the first $p-1$ components of U_i follow a multivariate sub-Gaussian distribution with mean zero and covariance matrix Σ_U . This implies that $v_i = (v_{i1}, \dots, v_{ip})^\top$ follows a logistic sub-Gaussian distribution (Aitchison and Shen, 1984) with the scale-invariance property: if v_i satisfies this distribution, so does any positive scalar multiple cv_i for $c > 0$, ensuring \tilde{X}_i satisfies the unit-sum constraint.

For tree-aggregated data, we write $U_A := UA$ and $\tilde{Z}_A := \tilde{Z}A$, yielding $\tilde{Z}_A = Z_A + U_A$. Each row of U_A has a multivariate sub-Gaussian distribution with covariance matrix $\Sigma_{U,A} = A^\top(\mathbf{I}_{p-1}, \mathbf{0}_{p-1})^\top \Sigma_U (\mathbf{I}_{p-1}, \mathbf{0}_{p-1})A$, where $\mathbf{0}_{p-1} = (0, \dots, 0)^\top \in \mathbb{R}^{p-1}$ and \mathbf{I}_{p-1} is the $(p-1) \times (p-1)$ identity matrix.

When replicate measurements are available, a natural estimator for the measurement-error covariance Σ_U is the unbiased sample covariance matrix of Carroll et al. (2006). In our framework,

Σ_U is a nuisance parameter; Section 3 shows that replacing Σ_U by any consistent estimator leaves all theoretical results intact.

2.3 Why Naive Tree Aggregation Fails under Contamination

Before introducing correction, we formalize the aggregation structure in the γ -parameterization and show why direct substitution of contaminated covariates leads to systematic bias.

Let β^* denote the true coefficient vector in (2), and let \mathcal{T} be a prespecified tree on the p compositional parts. We seek to identify $\gamma^* = \gamma^*(\beta^*, \mathcal{T})$ and its associated structure \mathcal{T}_γ . We assume that γ^* contains s nonzero elements, indicating that the leaf nodes corresponding to nonzero elements of β^* can be grouped into s distinct aggregation groups. For each node k with $\gamma_k^* \neq 0$, the aggregation group is $\mathcal{G}_k = L(\mathcal{T}_k)$, where $L(\mathcal{T}_k)$ denotes the leaf nodes within the subtree rooted at node k .

We initialize $\gamma_{0,k}^* = \beta_k^*$ for leaf nodes, $\gamma_{0,k}^* = 0$ for internal nodes, and $\mathcal{T}_{\gamma,0} = \mathcal{T}$. The aggregation process then proceeds iteratively from leaves toward the root, merging variables with identical effects into their common ancestor nodes.

Definition 1 (Aggregation process). *Let \mathcal{G} be the child set of a non-leaf node N_0 . If all $k \in \mathcal{G}$ have identical γ_k^* values, set $\gamma_k^* = 0$ for all $k \in \mathcal{G}$, assign $\gamma_{N_0}^* = \gamma_k^*$, and remove nodes \mathcal{G} from \mathcal{T}_γ .*

This yields $\mathcal{T}_\gamma \subseteq \mathcal{T}$, with nonzero γ^* values appearing only at the leaves of \mathcal{T}_γ . When $\mathcal{T}_\gamma \subsetneq \mathcal{T}$, the tree structure guides meaningful aggregation; when $\mathcal{T}_\gamma = \mathcal{T}$, no aggregation occurs, indicating that the tree \mathcal{T} and coefficient vector β^* are not aligned. For $\gamma^* = (\gamma_1^*, \dots, \gamma_T^*)^\top$, if node k is the nearest common ancestor of some group \mathcal{G}_u , then $\gamma_k^* = \beta_j^*$ for any $j \in \mathcal{G}_u$; otherwise, $\gamma_k^* = 0$.

Figure 1(a) illustrates this process with a tree \mathcal{T} having 3 leaves and 4 non-root nodes. Given $\gamma_1^* = \gamma_2^* = 0.5$ and nodes 1 and 2 sharing parent node 4, we aggregate nodes 1 and 2 into node 4 by setting $\gamma_4^* = 0.5$ and $\gamma_1^* = \gamma_2^* = 0$. Nodes 1 and 2 are then removed from \mathcal{T}_γ .

The aggregation process ensures that γ^* satisfies several desirable properties. First, it preserves the original model through the constraint $A\gamma^* = \beta^*$. Second, it minimizes the number of nonzero elements among all feasible candidates, providing the most parsimonious representation and motivating a sparsity-inducing penalty on γ . Third, each root-to-leaf path contains at most one nonzero element, facilitating the identification of distinct aggregation groups. For any tree \mathcal{T} and coefficient vector β^* , this process yields a unique γ^* , ensuring identifiability.

Given this aggregation structure, when only contaminated data \tilde{Z} is available, naive approaches

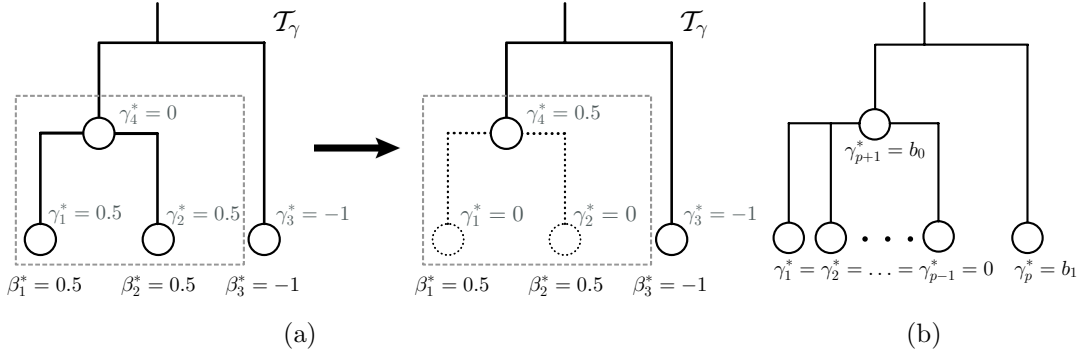


Figure 1: (a) Aggregation process: with $\beta^* = (0.5, 0.5, -1)^\top$, initialize $\gamma^* = (0.5, 0.5, -1, 0)^\top$ and $\mathcal{T}_\gamma = \mathcal{T}$; aggregating leaves 1–2 (gray dashed box) into node 4 yields $\gamma^* = (0, 0, -1, 0.5)^\top$ and the final \mathcal{T}_γ (solid lines). (b) Tree with first $p - 1$ leaves aggregated.

substitute \tilde{Z} for Z , leading to

$$\Psi_{\text{naive}} = n^{-1} A^\top \tilde{Z}^\top \tilde{Z} A = n^{-1} \tilde{Z}_A^\top \tilde{Z}_A \quad \text{and} \quad \psi_{\text{naive}} = n^{-1} A^\top \tilde{Z}^\top y = n^{-1} \tilde{Z}_A^\top y.$$

The naive estimator is then

$$\hat{\gamma}_{\text{naive}} = \arg \min_{\gamma} \left\{ \frac{1}{2} \gamma^\top \Psi_{\text{naive}} \gamma - \psi_{\text{naive}}^\top \gamma + \lambda \mathcal{P}(\gamma) \right\}, \quad \text{subject to } (A^\top \mathbf{1}_p)^\top \gamma = 0.$$

Under model (8), this estimator suffers from bias because

$$\mathbb{E}(n^{-1} \tilde{Z}^\top \tilde{Z}) = \mathbb{E}(n^{-1} Z^\top Z) + (\mathbf{I}_{p-1}, \mathbf{0}_{p-1})^\top \Sigma_U (\mathbf{I}_{p-1}, \mathbf{0}_{p-1}) \geq \mathbb{E}(n^{-1} Z^\top Z).$$

Tree aggregation amplifies this bias in a structured manner. Because aggregated features combine multiple leaf-level measurements, errors accumulate as one moves toward the root. The following proposition formalizes this phenomenon.

Proposition 1. *Let the rows of Z and U be sub-Gaussian with parameters τ_z^2 and τ^2 , respectively. For all $1 \leq k, l \leq T$, let $\tilde{\sigma}_{kl}$ denote the (k, l) th element of $\Sigma_{U, A}$. Then for any $\max\{(\tilde{\sigma}_{kl} - c_1 |L_k| |L_l| \tau \tau_z) / 2, 0\} < \epsilon \leq \min\{c_2 |L_k| |L_l| \tau \tau_z, \tilde{\sigma}_{kl} / 2\}$, we have*

$$P(|\Psi_{\text{naive}, kl} - \Psi_{kl}| > \epsilon) \geq 1 - 6 \exp \left[- \frac{c_3 n \min\{(2\epsilon - \tilde{\sigma}_{kl})^2, \epsilon^2\}}{|L_k|^2 |L_l|^2 \max\{\tau^2 \tau_z^2, \tau^4\}} \right].$$

Proposition 1 shows that the deviation depends on the aggregated error covariance entry $\tilde{\sigma}_{kl}$ and that the concentration rate deteriorates through the $|L_k|^2 |L_l|^2$ term in the denominator of the exponent. Under the working covariance structure in Section G of the Supplement, $|\tilde{\sigma}_{kl}|$ grows on the order of $|L_k| |L_l|$, so higher-level nodes with larger descendant leaf sets face a larger effective

noise scale, which is statistically analogous to a smaller effective sample size for those entries. This motivates TARCO’s use of leaf-count normalization in the stabilization step: without this scaling, a small number of high-level entries with large $|L_k||L_l|$ may dominate the optimization geometry.

To intuitively show how measurement errors propagate through tree structures, we analyze a simplified setting in which the first $p - 1$ leaves aggregate to a single parent node (Figure 1(b)). Under the working assumption that logarithmic errors share a common variance τ^2 and are pairwise uncorrelated, we derive closed-form expressions for the bias of the naive estimator. This analysis reveals that bias redistributes between parent and child nodes depending on τ^2 and the number of aggregated leaves: as measurement error variance increases, a greater proportion of bias shifts to the parent node. Moreover, the naive estimator incorrectly assigns nonzero coefficients to leaf nodes whose true coefficients are zero. These findings motivate the tree-weighted correction in our method. Full derivations and a corollary specializing Proposition 1 to this setting appear in Section G of the Supplement.

2.4 Tree-Aggregated Regression with Correction for Observation Error

We now introduce the method of Tree-Aggregated Regression with Correction for Observation Error (TARCO) for handling measurement errors in high-dimensional compositional data with hierarchical structure.

At the population level, the ideal quantities for estimation are $\mathbb{E}(\Psi) = \mathbb{E}(n^{-1}Z_A^\top Z_A)$ and $\mathbb{E}(\psi) = \mathbb{E}(n^{-1}Z_A^\top y)$. With these oracle quantities, the population-level optimization problem is

$$\gamma_{\text{pop}}^* = \arg \min_{\gamma} \left\{ \frac{1}{2} \gamma^\top \mathbb{E}(\Psi) \gamma - \mathbb{E}(\psi)^\top \gamma + \lambda \mathcal{P}(\gamma) \right\}, \quad \text{subject to } (A^\top \mathbf{1}_p)^\top \gamma = 0,$$

where $\mathcal{P}(\gamma)$ is a sparsity-inducing penalty. Since Z is unobserved, we must construct sample-level estimators that correct for measurement error.

Given only the contaminated data \tilde{Z} , we construct bias-corrected estimates by subtracting the measurement error covariance:

$$\begin{aligned} \hat{\Psi} &= A^\top \left\{ \frac{1}{n} \tilde{Z}^\top \tilde{Z} - (\mathbf{I}_{p-1}, \mathbf{0}_{p-1})^\top \Sigma_U (\mathbf{I}_{p-1}, \mathbf{0}_{p-1}) \right\} A = \frac{1}{n} \tilde{Z}_A^\top \tilde{Z}_A - \Sigma_{U,A}, \\ \tilde{\psi} &= \frac{1}{n} A^\top \tilde{Z}^\top y = \frac{1}{n} \tilde{Z}_A^\top y. \end{aligned} \tag{9}$$

The corrected cross-product $\tilde{\psi}$ requires no adjustment because U and y are independent by assumption.

When $T > n$, the corrected matrix $\widehat{\Psi}$ may fail to be positive semidefinite. To ensure a well-defined quadratic objective, we project $\widehat{\Psi}$ onto the positive semidefinite cone. Specifically, we solve

$$\widetilde{\Psi} = \arg \min_{\Psi \succeq 0} \|W^{-1}(\widehat{\Psi} - \Psi)W^{-1}\|_{\max},$$

where $\|M\|_{\max} = \max_{k,l} |M_{kl}|$ is the element-wise maximum norm, and W is a diagonal weighting matrix with $W_{kk} = |L_k|$. This weighting reflects the tree structure: entries corresponding to nodes with more descendants receive proportionally less weight in the projection, acknowledging their higher intrinsic variability (Proposition 1). The projection can be computed via the alternating direction method of multipliers (Boyd et al., 2011; Datta and Zou, 2017).

The TARCO estimator is then defined as

$$\hat{\gamma} = \arg \min_{\gamma} \left\{ \frac{1}{2} \gamma^{\top} \widetilde{\Psi} \gamma - \widetilde{\psi}^{\top} \gamma + \lambda \mathcal{P}(\gamma) \right\}, \quad \text{subject to } (A^{\top} \mathbf{1}_p)^{\top} \gamma = 0, \quad (10)$$

with the corresponding coefficient estimate $\hat{\beta} = A\hat{\gamma}$.

2.5 Penalty Choice and Computation

The penalty $\mathcal{P}(\gamma)$ can be tailored to incorporate prior knowledge about signal structure in the tree. We consider two choices. The first choice, weighted ℓ_1 penalty (Bien et al., 2021), is defined as $\mathcal{P}(\gamma) = \sum_{k=1}^T |L_k|^{\alpha} |\gamma_k|$, where the parameter α controls the sparsity pattern. Setting $\alpha = 0$ recovers the standard ℓ_1 penalty; $\alpha > 0$ encourages sparsity at upper nodes (favoring aggregation at leaves); and $\alpha < 0$ encourages sparsity at lower nodes (favoring aggregation at internal nodes). The second choice, descendant penalty (Li et al., 2023), is defined as $\mathcal{P}(\gamma) = \sum_{k=1}^T \|\gamma_j\|_{j \in \text{Desc}(k)}\|_1$, where $\text{Desc}(k)$ denotes the set of descendants of node k . This penalty promotes group sparsity among descendants, which is useful when signals concentrate within specific branches of the tree.

The optimization problem (10) is convex with linear constraints and can be solved using standard convex programming software such as CVXR (Fu et al., 2020). The regularization parameter λ is selected by cross-validation: the data are partitioned into K folds, and for each candidate λ , the model is fit on $K - 1$ folds and evaluated on the held-out fold. The value of λ minimizing the bias-corrected quadratic loss is selected; see Section J of the Supplement for more details.

For notational convenience, we use the p th component as the ALR reference. This requires $X_{ip} > 0$ almost surely so that the transformation is well defined. In practice, we choose a relatively abundant component as reference to reduce the chance of zeros and use a small pseudocount

when needed. Under this choice, the modeling assumptions remain practically reasonable in both simulation and application settings.

Changing the ALR reference is equivalent to applying an invertible linear transformation to the $(p - 1)$ -dimensional ALR vector, so the sub-Gaussian assumptions are preserved up to constants. At the estimation level, the estimator defined by (4) is reference-invariant (Lin et al., 2014). The positive semidefinite projection step can depend on the transformed coordinates, but Lemma 1 controls this effect by bounding the gap between projected and unprojected bias-corrected quantities. Therefore, our conclusions are driven primarily by problem dimension and tree structure rather than by a particular reference choice.

3 Theoretical Properties

3.1 Notation and Preliminaries

Let S denote the support of γ^* with cardinality $s = |S|$, and let S^c denote its complement. Write $S_{\setminus p} = S \setminus \{p\}$. Define $W = \text{diag}(|L_1|, \dots, |L_T|)$ and $W^\alpha = \text{diag}(|L_1|^\alpha, \dots, |L_T|^\alpha)$, where W_S is the diagonal submatrix indexed by S . Under the sum-to-zero constraint $\mathbf{1}_T^\top W \gamma = 0$, there exists a matrix $B \in \mathbb{R}^{T \times (T-1)}$ such that $\gamma = B \gamma_{\setminus p}$. For matrix indexing, we use M_{S,S^c} , $B_{I,J}$, $B_{:,J}$, and $B_{I,:}$ in the usual row-column sense. We write $G = \|\gamma^*\|_\infty$ and $\delta(s, p) = \sum_{j \in S} |L_j|$; $\delta(s, p)$ is an effective leaf-mass of the active set, equal to s when active nodes are leaves and larger when active nodes lie higher in the tree. The rows of Z and U are sub-Gaussian with variance proxies τ_z^2 and τ^2 , respectively, and we denote the covariance matrices of the first $p - 1$ columns by Σ_Z and Σ_U . The measurement error U has mean zero, and Σ_U is assumed known; Corollary 1 shows that substituting a consistent estimator leaves all results intact. The model error e has variance σ^2 . Additional constants φ , η , κ , and p_0 are introduced in Conditions 1 and 2.

Because both the measurement-error covariance Σ_U and the tree aggregation weights enter through leaf counts $|L_k|$, our bounds reflect the error amplification in Proposition 1. The theory has three components: Lemma 1 gives concentration of corrected quantities, Theorem 1 gives prediction and estimation bounds, and Theorem 2 gives sign consistency.

3.2 Theoretical Results

We first establish that the bias-corrected estimates (9) concentrate around their oracle sample counterparts.

Lemma 1 (Closeness Condition). Define $\epsilon_1 = c_3 \min\{\tau\sigma, \tau\tau_z\delta(s, p)G\}$ and $\epsilon_2 = c_4 \min\{\tau^2, \tau\tau_z\}$. For all $0 < \epsilon \leq \epsilon_1$,

$$P(|\tilde{\psi}_k - \psi_k| \leq |L_k|\epsilon) \geq 1 - 4s \exp(-c_5 n \epsilon^2 \zeta_1^{-1}),$$

where $\zeta_1 = \max\{\tau^2\sigma^2, \tau^2\tau_z^2\delta^2(s, p)G^2\}$. For all $0 < \epsilon \leq \epsilon_2$,

$$P(|\widehat{\Psi}_{kl} - \Psi_{kl}| \leq |L_k||L_l|\epsilon) \geq 1 - 6 \exp(-c_6 n \epsilon^2 \zeta_2^{-1}),$$

where $\zeta_2 = \max\{\tau^2\tau_z^2, \tau^4\}$.

Lemma 1 implies consistency of the corrected quantities, with deviation scale proportional to $|L_k||L_l|$, matching the tree-induced heterogeneity in Proposition 1.

To derive prediction error bounds, we impose a restricted eigenvalue condition analogous to that in van de Geer and Bühlmann (2009).

Condition 1 (Restricted Eigenvalue Condition). There exists a constant $\varphi > 0$ such that, for all nonzero $\gamma \in \mathcal{C}(S; 3, \alpha)$,

$$\gamma^\top \mathbb{E}(\Psi)\gamma \geq \varphi \|W^\alpha \gamma\|_2^2,$$

where $\mathcal{C}(S; 3, \alpha) = \{\gamma : \mathbf{1}_T^\top W\gamma = 0, \|W_{S^c}^\alpha \gamma_{S^c}\|_1 \leq 3 \|W_S^\alpha \gamma_S\|_1\}$.

This condition is imposed on $\mathbb{E}(\Psi)$, and its stringency depends on α .

Theorem 1 (Prediction Error Bound). Assume Condition 1 holds. Define $L_{\max}(\alpha) = \max_k (|L_k|^{1-\alpha})$ and $L_{\min}(\alpha) = \min_k (|L_k|^{1-\alpha})$. If the tuning parameter satisfies

$$C_1 L_{\max}(\alpha) \sqrt{\frac{\log T}{n}} \left(\sqrt{\zeta_1} + G\delta(s, p) \sqrt{\zeta_2} + \tau_z \sigma \right) \leq \lambda \leq C_2 L_{\min}(\alpha) \min\{\epsilon_1, G\delta(s, p)\epsilon_2, \tau_z \sigma\}, \quad (11)$$

and the restricted eigenvalue constant satisfies

$$C_3 (\tau_z^2 + \sqrt{\zeta_2})^{-1} (L_{\max}(\alpha))^2 s \sqrt{\frac{\log T}{n}} \leq \varphi \leq C_4 (L_{\min}(\alpha))^2 \min\{\tau_z^2, \epsilon_2\} s, \quad (12)$$

then with probability at least $1 - T^{-c}$,

$$\frac{\|Z\hat{\beta} - Z\beta^*\|_2^2}{n} \leq \frac{C_5 s}{\varphi} \lambda^2, \quad \|W^\alpha(\hat{\gamma} - \gamma^*)\|_1 \leq \frac{C_6 s}{\varphi} \lambda, \quad \|\hat{\beta} - \beta^*\|_1 \leq \frac{C_7 s}{\varphi} \lambda L_{\max}(\alpha).$$

Theorem 1 highlights a trade-off in α : larger α favors upper-level sparsity but makes Condition 1 harder to satisfy. The bounds simplify when $\alpha = 1$ or when leaf sizes are uniformly bounded ($|L_k| \leq L_0$). Under these scenarios, if $\zeta_1/\delta^2(s, p)$, ζ_2 , ϵ_1 , and ϵ_2 are $\mathcal{O}(1)$ and $\delta(s, p)\sqrt{\log(T)/n} \rightarrow 0$,

the intervals in (11)–(12) are non-degenerate; for a single-layer tree this reduces to the classical condition $s\sqrt{\log p/n} \rightarrow 0$ (Bickel et al., 2009; van de Geer and Bühlmann, 2009; Datta and Zou, 2017).

For sign consistency, we assume $p \in S = \text{supp}(\gamma^*)$ and impose an irrerepresentable condition analogous to classical Lasso settings (Zhao and Yu, 2006; Lin et al., 2014). This assumption is used for the primal-dual witness construction, since $p \notin S$ leads to a non-unique ℓ_1 subgradient at coordinate p . In typical applications this is mild: when $S \cap \{1, \dots, p\} \neq \emptyset$, one can relabel components so the ALR reference is an active leaf; the case with no active original leaves is outside our scope.

Condition 2 (Irrepresentable and Minimum Eigenvalue Condition). *The matrix $B_{S, S \setminus p}^\top \mathbb{E}(\Psi_{S, S}) B_{S, S \setminus p}$ is invertible with $\eta = \|(B_{S, S \setminus p}^\top \mathbb{E}(\Psi_{S, S}) B_{S, S \setminus p})^{-1}\|_\infty$. There exists $0 < \kappa < 1$ such that*

$$\|W_{S^c}^{-\alpha} \{B_{:, S^c}^\top \tilde{\Psi} B_{:, S \setminus p} (B_{:, S \setminus p}^\top \tilde{\Psi} B_{:, S \setminus p})^{-1} B_{S, S \setminus p}^\top W_S^\alpha \text{sign}(\gamma_S^*) + |L_p|^{\alpha-1} \text{sign}(\gamma_p^*) W_{S^c} \mathbf{1}_{T-S}\} \|_\infty < 1 - \kappa$$

with probability at least $1 - p_0(n, s, T)$.

Because Ψ is random, the second requirement is probabilistic, with failure probability summarized by $p_0(n, s, T) \rightarrow 0$. Note that p is the ALR reference leaf node, so $|L_p| = 1$; we retain the factor $|L_p|^{\alpha-1}$ for notational homogeneity with the KKT expressions in Section E of the Supplement.

Theorem 2 (Sign Consistency). *Assume Condition 2 holds. Define $L_{S, \max}(\alpha) = \max_{k \in S} |L_k|^{1-\alpha}$, $L_{S, \min}(\alpha) = \min_{k \in S} |L_k|^{1-\alpha}$, and let $C_\Pi = \|\Pi\|_\infty$ for the projection $\Pi = I - \tilde{\Psi} B_{:, S \setminus p} (B_{:, S \setminus p}^\top \tilde{\Psi} B_{:, S \setminus p})^{-1} B_{:, S \setminus p}^\top$. If the tuning parameter satisfies*

$$\begin{aligned} C_9 \max \left\{ L_{S, \max}(\alpha), \kappa^{-1} C_\Pi L_{\max}(\alpha) L_{\max}(0) \right\} \sqrt{\frac{\log T}{n}} \left(\sqrt{\zeta_1} + G\delta(s, p) \sqrt{\zeta_2} + \tau_z \sigma \right) &\leq \lambda \\ &\leq C_{10} \min \left\{ L_{S, \min}(\alpha), \kappa^{-1} C_\Pi L_{\max}(\alpha) \right\} \min \{ \epsilon_1, G\delta(s, p) \epsilon_2, \tau_z \sigma \}, \end{aligned}$$

and

$$C_{11} (\sqrt{\zeta_2} + \tau_z) s \delta(s, p) \sqrt{\frac{\log T}{n}} \leq (\eta L_{S, \max}(0))^{-1} \leq C_{12} s \delta(s, p) \min \{ \epsilon_2, \tau_z^2 \},$$

then with probability at least $1 - T^{-c} - p_0(n, s, T)$:

1. $\|\hat{\gamma}_S - \gamma_S^*\|_\infty \leq 3\lambda\eta\delta(s, p) \max_{k \in S} (|L_k|^\alpha + |L_k|)$.
2. If $\gamma_{\min}^* = \min_{k \in S} |\gamma_k^*| > 3\lambda\eta\delta(s, p) \max_{k \in S} (|L_k|^\alpha + |L_k|)$, then $\text{sign}(\hat{\gamma}) = \text{sign}(\gamma^*)$.

The proof centers on three tasks: invertibility of $B_{:,S_{\setminus p}}^\top \tilde{\Psi} B_{:,S_{\setminus p}}$, control of its norm, and strict dual feasibility. Under $\alpha = 1$, bounded leaf size ($|L_k| \leq L_0 = \mathcal{O}(1)$), and $\eta, \kappa, C_\Pi = \mathcal{O}(1)$ with $p_0(n, s, T) = \mathcal{O}(T^{-c})$, sign consistency follows when

$$\delta^2(s, p) \sqrt{\frac{\log T}{n}} \rightarrow 0$$

and the minimum signal strength satisfies

$$\gamma_{\min}^* > C_{13} \delta^2(s, p) \sqrt{\frac{\log T}{n}}.$$

These requirements reflect the additional difficulty of sign recovery under random design, tree structure, and ALR transformation.

All preceding results assume Σ_U is known. When it must be estimated from replicates, the guarantees remain valid.

Corollary 1. *Suppose t_i replicate measurements $\tilde{\mathbf{Z}}_{i1}, \dots, \tilde{\mathbf{Z}}_{it_i}$ are available for each sample i , and define*

$$\hat{\Sigma}_U = \frac{\sum_{i=1}^n \sum_{t=1}^{t_i} (\tilde{\mathbf{Z}}_{it} - \bar{\mathbf{Z}}_i)(\tilde{\mathbf{Z}}_{it} - \bar{\mathbf{Z}}_i)^\top}{\sum_{i=1}^n (t_i - 1)}. \quad (13)$$

If there exists a constant C_{14} independent of n such that $\max_i (t_i - 1) \leq C_{14} \sum_{i=1}^n (t_i - 1)/n$, then Lemma 1, Theorem 1, and Theorem 2 continue to hold with $\hat{\Sigma}_U$ in place of Σ_U .

In summary, TARCO achieves prediction and sign-recovery guarantees under tree-aware error amplification, and the same guarantees hold with $\hat{\Sigma}_U$ when replicates are available.

4 Simulation studies

We evaluate TARCO under various penalty structures through simulation. For the weighted ℓ_1 penalty $\sum_{k=1}^T |L_k|^\alpha |\gamma_k|$, we consider $\alpha = 0$ (TARCO), $\alpha = 0.5$ (TARCO-05), and $\alpha = -0.5$ (TARCO-n05). We also consider the descendant-group penalty $\mathcal{P}(\gamma) = \sum_{k=1}^T \|(\gamma_j)_{j \in \text{Desc}(k)}\|_1$, (TARCO-Des). For comparison, we include tree-aggregation of compositional data applied to corrupted observations (TRAC-Naive; [Bien et al., 2021](#)) and CoCoLasso (COCO; [Datta and Zou, 2017](#)).

4.1 Simulation settings

We generate compositional data $X = (X_{ij}) \in \mathbb{R}^{n \times p}$ from a logistic-normal distribution following [Lin et al. \(2014\)](#), with $n = 100$ and $p = 100$. Specifically, we first draw $W = (w_{ij}) \in \mathbb{R}^{n \times p}$

from a multivariate normal distribution with mean $\mu = (\mu_1, \dots, \mu_p)^\top$ and covariance $\Sigma_{ij} = \rho^{|i-j|}$, where $\rho = 0.5$. Following Li et al. (2023), we set $\mu_j = \log(p/2)$ for $j = 1, \dots, 5$ and $\mu_j = 0$ otherwise. The compositional data are then obtained via the softmax transformation $X_{ij} = \exp(w_{ij}) / \sum_{l=1}^p \exp(w_{il})$.

The log-ratio transformation yields $Z = \{\log(X_{ij}/X_{ip})\} \in \mathbb{R}^{n \times (p-1)}$, with the p th component as the reference. The measurement error matrix U is drawn from a multivariate normal distribution with mean zero and covariance Σ_U as specified in Section G of the Supplement, with $\tau = 1$. The corrupted data are $\tilde{Z} = Z + U$.

To estimate Σ_U , we generate paired replicates: for each sample, we create two copies sharing the same true Z but with independent realizations of \tilde{Z} . This yields $2n$ observations from which $\hat{\Sigma}_U$ is computed via (13). For TRAC-Naive, we recover the corrupted compositions \tilde{X} by inverting the log-ratio transformation. For COCO, we fit the model on (\tilde{Z}, y) to obtain a $(p-1)$ -dimensional estimate $\hat{\beta}_{\setminus p}$, then expand to dimension p using the constraint $\mathbf{1}_p^\top \hat{\beta} = 0$. The tuning parameter λ is selected by 5-fold cross-validation (Section J of the Supplement).

The true coefficient vector is $\beta^* = (0.5 \cdot \mathbf{1}_{20}^\top, -0.75 \cdot \mathbf{1}_{10}^\top, -0.25 \cdot \mathbf{1}_{10}^\top, 0.1 \cdot \mathbf{1}_{20}^\top, -0.1 \cdot \mathbf{1}_{20}^\top, \mathbf{0}_{15}^\top, \nu_5^\top)^\top$, where $\mathbf{1}_q$ denotes a vector of q ones and $\nu_5 \in \mathbb{R}^5$ is drawn from $N(0, 0.25I_5)$ and then centered. This structure reflects the tree in Figure 2: the first 20 features share a common ancestor, as do features 21–30, and so forth. The terms $\pm 0.1 \cdot \mathbf{1}_{20}$ represent weak but broadly aggregating signals, while ν_5 captures random leaf-level effects. The coefficient vector satisfies $\mathbf{1}_p^\top \beta^* = 0$ and corresponds to $s = 11$ aggregation groups. Responses are generated from the linear model (2) with $\sigma = 0.5$.

We assess performance using three metrics. Mean squared prediction error, $\text{MSPE}(\hat{\beta}) = \|y_{\text{test}} - Z_{\text{test}} \hat{\beta}\|_2^2 / n$, measures predictive accuracy on an independent test set of the same size as the training data. Absolute error, $\text{AE}(\hat{\beta}) = \|\hat{\beta} - \beta^*\|_1$, quantifies estimation accuracy. Group recovery, $\text{GR}(\hat{\beta}) = (\text{TP} + \text{TN}) / \binom{p}{2}$, is the Rand index (Rand, 1971; Hubert and Arabie, 1985) for recovering aggregation structure. To evaluate group recovery at a coarse structural level, we construct a reference partition by applying one-dimensional k-means clustering with $K = 5$ to β^* , and for each estimate $\hat{\beta}$ we apply the same procedure to obtain an estimated partition. The counts TP and TN are then computed over all unordered pairs (i, j) by comparing whether the two partitions place the pair in the same group or in different groups. The same clustering rule is used for all competing methods. Results are based on 100 Monte Carlo replicates.

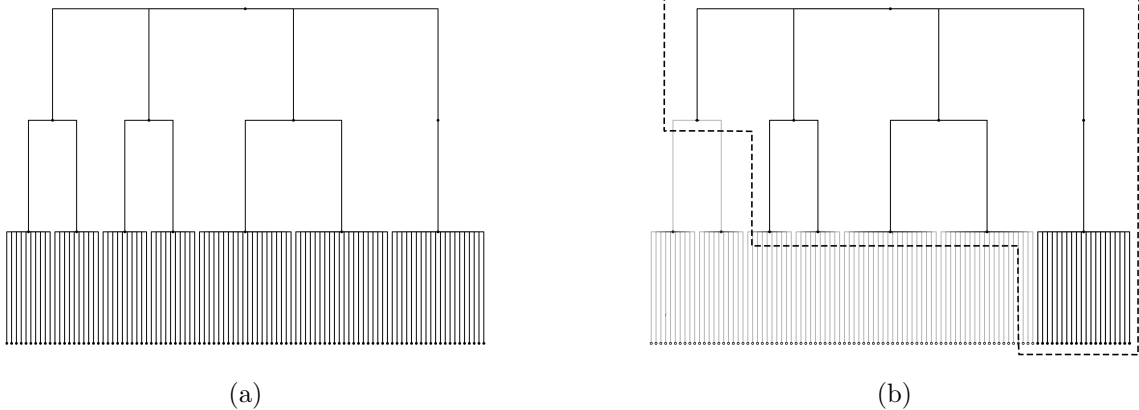


Figure 2: Tree structure used in simulations. Left: the full tree \mathcal{T} with $p = 100$ leaves. Right: the aggregated tree \mathcal{T}_γ (dashed box) induced by the true coefficients β^* .

4.2 Simulation results

Table 1 summarizes the results across sample-size and dimensionality regimes. In the baseline setting ($n = 100, p = 100$), all TARCO variants outperform TRAC-Naive, which ignores measurement error, and COCO, which corrects for measurement error but does not exploit tree structure. Among TARCO variants, TARCO, TARCO-n05, and TARCO-Des achieve the lowest prediction and estimation errors and the highest group recovery, whereas TARCO-05 performs less well, likely because the large number of leaves relative to internal nodes favors aggregation toward leaves rather than the root. In the higher-dimensional setting ($n = 100, p = 200$), all methods show higher MSPE and AE, but TARCO and TARCO-n05 maintain clear advantages over TRAC-Naive and COCO. In the large-sample setting ($n = 500, p = 100$), performance gaps widen further: TARCO variants improve substantially, while gains for TRAC-Naive and COCO are more modest.

We also examine robustness to model misspecification by setting 20% of coordinates of β^* to zero at regular intervals, creating leaf nodes with no true effect and partially breaking tree-signal alignment. Despite this challenge, TARCO methods remain stable (Table 1, Misspecified). We omit GR in this setting because the group structure is no longer well defined. Additional simulations varying the signal-to-noise ratio τ/τ_z are reported in Section H of the Supplement; TARCO methods remain stable across a wide range of values.

Table 1: Simulation results across settings. Entries are mean (SD) over 100 replicates.

Metric	TARCO	TARCO-05	TARCO-n05	TARCO-Des	TRAC-Naive	COCO
$p = 100, n = 100$						
MSPE	2.52 (0.91)	3.60 (1.25)	2.11 (0.72)	2.73 (0.98)	3.93 (1.14)	18.94 (6.70)
AE	7.43 (1.58)	9.82 (1.68)	6.62 (1.40)	7.56 (1.67)	9.30 (1.48)	23.76 (1.86)
GR	0.95 (0.06)	0.87 (0.05)	0.98 (0.04)	0.95 (0.06)	0.91 (0.07)	0.41 (0.07)
$p = 200, n = 100$						
MSPE	4.56 (1.67)	8.44 (2.99)	3.95 (1.36)	4.53 (1.58)	7.34 (2.50)	52.40 (12.10)
AE	13.85 (2.80)	20.81 (3.20)	12.96 (2.46)	13.63 (2.40)	17.50 (3.31)	49.43 (2.22)
GR	0.96 (0.06)	0.88 (0.05)	0.97 (0.05)	0.96 (0.05)	0.93 (0.07)	0.35 (0.07)
$p = 100, n = 500$						
MSPE	1.19 (0.29)	1.45 (0.32)	1.17 (0.28)	1.31 (0.29)	2.99 (0.40)	6.63 (1.35)
AE	4.72 (1.19)	6.08 (1.19)	4.57 (1.23)	5.06 (1.30)	8.34 (0.70)	19.22 (2.07)
GR	0.98 (0.03)	0.95 (0.06)	0.98 (0.03)	0.98 (0.03)	0.95 (0.05)	0.57 (0.04)
Misspecified						
MSPE	2.11 (0.36)	2.25 (0.34)	2.13 (0.37)	1.90 (0.32)	3.03 (0.34)	4.82 (0.98)
AE	9.62 (0.92)	10.72 (0.86)	9.44 (0.90)	8.68 (0.92)	11.30 (0.54)	15.20 (1.77)

5 Applications

We apply TARCO to data from a microbiome study (Flores et al., 2014), in which participants provided weekly gut microbiome samples over three months along with lifestyle variables including health status, medication use, and menstrual cycles. Our goal is to assess the association between body mass index (BMI) and microbiome composition.

After excluding individuals with missing BMI data and retaining only the four most similar samples per participant based on community composition dissimilarity (Shi et al., 2022; Zhao and Wang, 2024), the final dataset comprises 160 samples from 40 participants. Following Shi et al. (2022), we treat these within-participant samples as approximate replicates for estimating the ALR-scale error covariance. Because these are biological repeats rather than technical replicates, the estimated covariance should be interpreted as capturing measurement variability and short-term within-participant fluctuations. Accordingly, the regression coefficients are interpreted as associations with participant-level latent composition after averaging short-term temporal variation. Microbial abundances were recorded at the genus level, covering 89 taxa with an accompanying phylogenetic tree from the Genome Taxonomy Database (Parks et al., 2022). The tree spans taxonomic ranks from genus to kingdom.

A pseudocount of 0.1 was added to each zero entry in the raw count data prior to normaliza-

tion, following standard practice in compositional data analysis (Aitchison, 1982; Martín-Fernández et al., 2000; Lin et al., 2014; Kaul et al., 2017). The most abundant genus, *Bacteroides* (mean relative abundance 32.1%), served as the ALR reference. We partitioned the data into a baseline set of 40 samples (one per participant) for estimating regression coefficients and a secondary set of 120 samples (three per participant) for estimating measurement-error parameters. Results from TARCO are compared with TRAC-Naive and COCO, with additional methods reported in Section I of the Supplement. We also assessed sensitivity to ALR reference choice and found stable qualitative conclusions: using alternative reference taxa produced consistent key selected groups and association directions, with only minor changes in coefficient magnitudes. A representative analysis using genus *Butyrivibrio* as the reference is reported in Section I of the Supplement.

Figure 3 displays the phylogenetic tree alongside estimated coefficients for each method. Bars on the outer ring represent coefficient magnitudes, with taxa aggregated at common ancestors when their estimates are similar. TARCO yields more coherent aggregation than the alternatives. Specifically, TARCO identifies positive associations between BMI and *Megamonas* (genus), *Desulfovibrionaceae* (family), *Lactobacillales* (order), and *Butyrivibrio* (genus), and negative associations with *Gammaproteobacteria* (class), *Veillonellales* (order), and *Marinifilaceae* (family). Among these, *Megamonas* and *Butyrivibrio* are selected by all three methods, while *Veillonellales* is selected by both TARCO and TRAC-Naive. TRAC-Naive also selects *Moraxellaceae*, a descendant of *Gammaproteobacteria*.

These findings align with existing literature. *Megamonas* is enriched in higher-BMI cohorts, with mechanistic evidence that certain strains promote adiposity (Wu et al., 2024). *Gammaproteobacteria*, particularly its descendant order *Enterobacterales*, has been negatively associated with BMI (Hu et al., 2022; Legrand et al., 2020). *Veillonellales* correlates with obesity and adiposity metrics (Peters et al., 2018), while *Desulfovibrionaceae* is elevated in obese patients and linked to adverse metabolic phenotypes (Lin et al., 2022). Several *Lactobacillus* species within *Lactobacillales* have been associated with obesity (Crovesy et al., 2017; Hu et al., 2022). *Butyrivibrio* is associated with healthier metabolic profiles (Peng et al., 2023), and *Bacteroidales*, the ancestral order of *Marinifilaceae*, predicts weight loss on fiber-rich diets (Hjorth et al., 2019).

6 Discussion

We introduced TARCO, a method for log-contrast regression with tree-structured features under measurement error. Starting from a multiplicative error model on pre-compositional quantities,

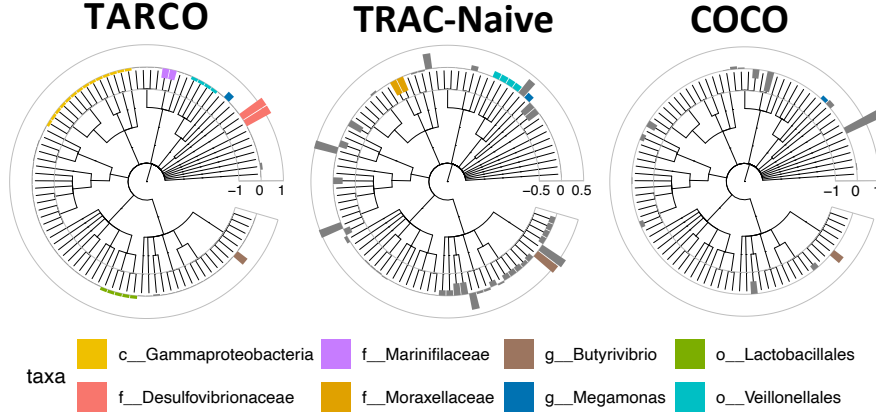


Figure 3: Phylogenetic tree of the 89 genera analyzed and the corresponding coefficient estimates. Taxa aggregated at common ancestors are indicated by matching colors.

we showed that the additive log-ratio transformation converts these errors to an additive form. TARCO corrects the score vector, adjusts the Gram matrix, and projects it onto a tree-weighted positive semidefinite cone. Our theoretical analysis characterizes how measurement error propagates through the tree hierarchy, establishes finite-sample prediction bounds, and provides conditions for sign consistency. Simulations and an application to gut microbiome data confirm that TARCO yields both accurate predictions and interpretable aggregations.

The framework accommodates structured regularization aligned with scientific objectives. Weighted ℓ_1 penalties and descendant-group penalties can promote sparsity at selected tree levels and steer aggregation toward meaningful internal nodes, reducing noise from rare leaves while highlighting pathway- or module-level signals. The correction and regularization steps are modular, allowing other convex penalties to be incorporated without modification.

Several directions merit further investigation. First, zero values are prevalent in compositional data. While replacing zeros with small constants is common practice (Martín-Fernández et al., 2000), a zero-aware model that explicitly connects the pre-compositional error process to the ALR scale would be more principled. Second, penalty selection remains an open problem; data-driven choice of penalty type and weights, including adaptive leaf-count scaling, would improve robustness for trees with heterogeneous depth. Third, tree uncertainty matters in applications where the hierarchy is itself estimated. Sensitivity analysis with respect to local tree modifications, or joint learning of coarse merges and regression coefficients, would extend the method’s applicability. Finally, when replicate measurements are limited, plug-in estimators of the measurement-error covariance can be unstable. Shrinkage toward the ALR-induced structure, combined with sensitivity

checks on τ^2 , could help stabilize estimation and inference.

Data availability statement

The data analyzed in this study were obtained from the supplementary materials of [Shi et al. \(2022\)](#). The data are publicly available via the publisher’s website.

Supplementary materials

The supplementary materials contain preliminary lemmas, proofs of all theoretical results, a toy example, additional simulation results, more comprehensive data analyses, and the detailed cross-validation procedure. R code for implementing the proposed method is available upon request during the revision process and will be released publicly on GitHub upon acceptance.

References

- Aitchison, J. (1982), ‘The statistical analysis of compositional data’, *Journal of the Royal Statistical Society: Series B (Methodological)* **44**(2), 139–160.
- Aitchison, J. and Bacon-Shone, J. (1984), ‘Log contrast models for experiments with mixtures’, *Biometrika* **71**(2), 323–330.
- Aitchison, J. and Shen, S. (1984), ‘Measurement error in compositional data’, *Journal of the International Association for Mathematical Geology* **16**, 637–650.
- Bickel, P. J., Ritov, Y. and Tsybakov, A. B. (2009), ‘Simultaneous analysis of Lasso and Dantzig selector’, *The Annals of Statistics* **37**(4), 1705–1732.
- Bien, J., Yan, X., Simpson, L. and Müller, C. L. (2021), ‘Tree-aggregated predictive modeling of microbiome data’, *Scientific Reports* **11**(1), 14505.
- Boyd, S., Parikh, N., Chu, E., Peleato, B., Eckstein, J. et al. (2011), ‘Distributed optimization and statistical learning via the alternating direction method of multipliers’, *Foundations and Trends® in Machine learning* **3**(1), 1–122.
- Carroll, R. J., Ruppert, D., Stefanski, L. A. and Crainiceanu, C. M. (2006), *Measurement error in nonlinear models: a modern perspective*, Chapman and Hall/CRC.

- Crovesy, L., Ostrowski, M., Ferreira, D., Rosado, E. and Soares-Mota, M. (2017), ‘Effect of lactobacillus on body weight and body fat in overweight subjects: a systematic review of randomized controlled clinical trials’, *International journal of obesity* **41**(11), 1607–1614.
- Datta, A. and Zou, H. (2017), ‘CoCoLasso for high-dimensional error-in-variables regression’, *The Annals of Statistics* **45**(6), 2400–2426.
- Firth, D. and Sammut, F. (2023), ‘Analysis of composition on the original scale of measurement’, *arXiv preprint arXiv:2312.10548*.
- Flores, G. E., Caporaso, J. G., Henley, J. B., Rideout, J. R., Domogala, D., Chase, J., Leff, J. W., Vázquez-Baeza, Y., Gonzalez, A., Knight, R. et al. (2014), ‘Temporal variability is a personalized feature of the human microbiome’, *Genome biology* **15**(12), 531.
- Fu, A., Narasimhan, B. and Boyd, S. (2020), ‘CVXR: An R package for disciplined convex optimization’, *Journal of Statistical Software* **94**(14), 1–34.
- Garcia, T. P., Müller, S., Carroll, R. J. and Walzem, R. L. (2014), ‘Identification of important regressor groups, subgroups and individuals via regularization methods: application to gut microbiome data’, *Bioinformatics* **30**(6), 831–837.
- Gihawi, A., Ge, Y., Lu, J., Puiu, D., Xu, A., Cooper, C. S., Brewer, D. S., Pertea, M. and Salzberg, S. L. (2023), ‘Major data analysis errors invalidate cancer microbiome findings’, *Mbio* **14**(5), e01607–23.
- Hjorth, M. F., Blædel, T., Bendtsen, L. Q., Lorenzen, J. K., Holm, J. B., Küllerich, P., Roager, H. M., Kristiansen, K., Larsen, L. H. and Astrup, A. (2019), ‘Prevotella-to-bacteroides ratio predicts body weight and fat loss success on 24-week diets varying in macronutrient composition and dietary fiber: results from a post-hoc analysis’, *International Journal of Obesity* **43**(1), 149–157.
- Hu, J., Guo, P., Mao, R., Ren, Z., Wen, J., Yang, Q., Yan, T., Yu, J., Zhang, T. and Liu, Y. (2022), ‘Gut microbiota signature of obese adults across different classifications’, *Diabetes, Metabolic Syndrome and Obesity: Targets and Therapy* pp. 3933–3947.
- Hubert, L. and Arabie, P. (1985), ‘Comparing partitions’, *Journal of classification* **2**, 193–218.

- Kaul, A., Mandal, S., Davidov, O. and Peddada, S. D. (2017), ‘Analysis of microbiome data in the presence of excess zeros’, *Frontiers in microbiology* **8**, 2114.
- Legrand, R., Lucas, N., Dominique, M., Azhar, S., Deroissart, C., Le Sollicec, M.-A., Rondeaux, J., Nobis, S., Guérin, C., Léon, F. et al. (2020), ‘Commensal hafnia alvei strain reduces food intake and fat mass in obese mice—a new potential probiotic for appetite and body weight management’, *International Journal of Obesity* **44**(5), 1041–1051.
- Li, G., Li, Y. and Chen, K. (2023), ‘It’s all relative: Regression analysis with compositional predictors’, *Biometrics* **79**(2), 1318–1329.
- Lin, W., Shi, P., Feng, R. and Li, H. (2014), ‘Variable selection in regression with compositional covariates’, *Biometrika* **101**(4), 785–797.
- Lin, Y.-C., Lin, H.-F., Wu, C.-C., Chen, C.-L. and Ni, Y.-H. (2022), ‘Pathogenic effects of desulfovibrio in the gut on fatty liver in diet-induced obese mice and children with obesity’, *Journal of gastroenterology* **57**(11), 913–925.
- Loh, P.-I. and Wainwright, M. J. (2011), High-dimensional regression with noisy and missing data: Provable guarantees with non-convexity, in ‘Advances in Neural Information Processing Systems’, Vol. 24, Curran Associates, Inc., pp. 765–773.
- Martín-Fernández, J., Barceló-Vidal, C. and Pawłowsky-Glahn, V. (2000), Zero replacement in compositional data sets, in ‘Data analysis, classification, and related methods’, Springer, pp. 155–160.
- Parks, D. H., Chuvochina, M., Rinke, C., Mussig, A. J., Chaumeil, P.-A. and Hugenholtz, P. (2022), ‘Gtdb: an ongoing census of bacterial and archaeal diversity through a phylogenetically consistent, rank normalized and complete genome-based taxonomy’, *Nucleic acids research* **50**(D1), D785–D794.
- Peng, K., Dong, W., Luo, T., Tang, H., Zhu, W., Huang, Y. and Yang, X. (2023), ‘Butyrate and obesity: Current research status and future prospect’, *Frontiers in Endocrinology* **14**, 1098881.
- Peters, B. A., Shapiro, J. A., Church, T. R., Miller, G., Trinh-Shevrin, C., Yuen, E., Friedlander, C., Hayes, R. B. and Ahn, J. (2018), ‘A taxonomic signature of obesity in a large study of american adults’, *Scientific reports* **8**(1), 9749.

- Rand, W. M. (1971), ‘Objective criteria for the evaluation of clustering methods’, *Journal of the American Statistical association* **66**(336), 846–850.
- Randolph, T. W., Zhao, S., Copeland, W., Hullar, M. and Shojaie, A. (2018), ‘Kernel-penalized regression for analysis of microbiome data’, *The annals of applied statistics* **12**(1), 540.
- Shi, P., Zhang, A. and Li, H. (2016), ‘Regression analysis for microbiome compositional data’, *The Annals of Applied Statistics* **10**(2), 1019–1040.
- Shi, P., Zhou, Y. and Zhang, A. R. (2022), ‘High-dimensional log-error-in-variable regression with applications to microbial compositional data analysis’, *Biometrika* **109**(2), 405–420.
- Silverman, J. D., Washburne, A. D., Mukherjee, S. and David, L. A. (2017), ‘A phylogenetic transform enhances analysis of compositional microbiota data’, *Elife* **6**, e21887.
- Tan, W., Xue, L., Yang, S. and Zhan, X. (2024), ‘High-dimensional log contrast models with measurement errors’, *arXiv preprint arXiv:2407.15084* .
- van de Geer, S. A. and Bühlmann, P. (2009), ‘On the conditions used to prove oracle results for the Lasso’, *Electronic Journal of Statistics* **3**, 1360–1392.
- Wang, T. and Zhao, H. (2017), ‘Structured subcomposition selection in regression and its application to microbiome data analysis’, *The Annals of Applied Statistics* **11**(2), 771–791.
- Wu, C., Yang, F., Zhong, H., Hong, J., Lin, H., Zong, M., Ren, H., Zhao, S., Chen, Y., Shi, Z. et al. (2024), ‘Obesity-enriched gut microbe degrades myo-inositol and promotes lipid absorption’, *Cell Host & Microbe* **32**(8), 1301–1314.
- Yan, X. and Bien, J. (2021), ‘Rare feature selection in high dimensions’, *Journal of the American Statistical Association* **116**(534), 887–900.
- Zhao, H. and Wang, T. (2024), ‘Debiased high-dimensional regression calibration for errors-in-variables log-contrast models’, *Biometrics* **80**(4), ujae153.
- Zhao, P. and Yu, B. (2006), ‘On model selection consistency of lasso’, *Journal of Machine learning research* **7**(Nov), 2541–2563.